Magnetic ordering and magnetocrystalline anisotropy in epitaxial Mn$_2$GaC MAX phase thin films

Einar B. Thorsteinsson[1], Arni S. Ingason[2], and Fridrik Magnus[1]

[1]*Science Institute, University of Iceland, Dunhaga 3, 107 Reykjavik, Iceland*
[2]*Grein Research ehf., Dunhaga 5, 107 Reykjavik, Iceland*

Mn$_2$GaC is a MAX phase belonging to a family of naturally nanolaminated materials with formula $M_{n+1}AX_n$ ($n = 1, 2, 3$), where M is a transition metal, A is an A-group element, and X is carbon or nitrogen. It has a complex magnetic phase diagram, and there are many open questions regarding its magnetic properties. Here we study epitaxial films of Mn$_2$GaC with two different crystal orientations on MgO(1 1 1) substrates: a (0 0 0 l) dominated orientation and a mixed (0 0 0 l) and (1 0 $\bar{1}$ 3) orientation. Magnetic measurements between 3 and 320 K are presented for in-plane and out-of-plane magnetic fields on both types of film, which show that Mn$_2$GaC has a magnetocrystalline anisotropy with (0 0 0 l) as easy planes. This provides clear experimental evidence of the anisotropic properties associated with the nanolaminated structure of a MAX phase. In addition, a close look at the magnetic response at low temperature shows that the noncollinear magnetic state is unchanged below 50 K, contrary to previous results, with a magnetic moment of 0.38 μ_B per Mn atom at a temperature of 3 K and applied field of 5 T.

I. INTRODUCTION

Low-dimensional magnetism has seen a surge in interest in recent years fueled by the discovery of an increasing number of layered van der Waals crystals [1–3]. The reduced dimensions and potential for competing interactions open up the possibility of exotic magnetic ordering beyond conventional ferro- or antiferromagnetism. MAX phases are another family of naturally nanolaminated materials composed of a transition metal (M), an A-group element (A), and either carbon or nitrogen (X) with the chemical formula $M_{n+1}AX_n$ ($n = 1, 2, 3$) [4]. They have an atomically layered structure which for $n = 1$ has the order M-A-M-X-M-A-M-X. The first magnetic MAX phase, (Cr$_{0.75}$Mn$_{0.25}$)$_2$GeC, was synthesized [5] in 2013, and since then a small number of other phases containing either Mn or Cr on the M site have shown interesting magnetic properties [6–11]. These properties arise due to the frustrated coupling between M-site atoms both within the M-X-M trilayers and across the A layers. Such frustrated magnetic systems can be a source of complex spin textures such as spin spirals and skyrmions, which could potentially be used in magnetic storage and logic devices [12].

In particular, Mn$_2$GaC has been shown to have a rich magnetic phase diagram which makes it of interest not only in magnetoelectric applications but also for magnetocalorics [6,11,13]. At low temperature it exhibits noncollinear antiferromagnetic ordering, and at ∼210 K it undergoes a magnetic phase transition to collinear antiferromagnetic ordering. The magnetic phase transition coincides with a structural phase transition, where an abrupt change in the c-axis lattice parameter takes place [6]. The coupled magnetic and structural phase transition can also be induced by applying a magnetic field at temperatures above 210 K. This complex magnetic behavior is a result of competing ferromagnetic and antiferromagnetic exchange interactions within and between the M layers as shown by first-principles calculations and Monte Carlo simulations. However, many questions remain about its magnetic ordering, particularly the noncollinear antiferromagnetic state at low temperature [14,15]. Furthermore, there has yet to be presented any experimental evidence of magnetocrystalline anisotropy in Mn$_2$GaC, despite its highly anisotropic nanolaminated structure [9,16]. Both subjects are important to gain the thorough understanding of this materials system which is necessary if its properties are to be tuned to a specific application.

Here we examine the magnetic ordering and anisotropy in epitaxial films of Mn$_2$GaC. We use two single-phase Mn$_2$GaC samples with different epitaxial relationships with the substrate to determine the presence of magnetocrystalline anisotropy. Furthermore, we carefully characterize the magnetic response of Mn$_2$GaC at low temperature in order to elucidate the low-temperature magnetic state.

II. EXPERIMENT

The films were grown by direct current magnetron sputtering (dcMS) on 1×1 cm^2 MgO(111) substrates from a 7.5-cm-diameter 99.9% manganese target, a 7.5-cm 99.99% carbon target, and a liquid gallium target made from 99.9999% gallium pellets. The Ga was held in a specially made 5.0-cm copper crucible which was mounted on a standard circular magnetron at the bottom of the vacuum chamber. During sputtering the Ga target was maintained in liquid form by limiting the flow of cooling water through the magnetron. The magnetrons were arranged in a confocal geometry with a target-substrate distance of approximately 160 mm. The sputtering was carried out in a 20-SCCM (cubic centimeters per minute at STP) flow of 99.999% purity argon gas using a throttle valve to adjust the pressure to 0.40 Pa. The vacuum chamber had a base pressure of below 5×10^{-7} Pa; however,

at the growth temperature of 550 °C the base pressure rose to 5×10^{-6} Pa. For the duration of the growth the sample holder was rotated by $\pm 360°$ at a rate of 12 rpm. The substrates were cleaned in an ultrasonic bath for 5 min in acetone followed by 5 min of ethanol and then annealed *in situ* in vacuum at 600 °C for 60 min immediately prior to growth.

The Mn and C growth rates were determined by growing single films of Mn and C and measuring thickness by x-ray reflectometry (XRR). This approach is not applicable to Ga due to its low melting point, and therefore its growth rate was estimated by growing a series of MnGa$_x$ films with a known Mn rate and performing composition analysis with energy dispersive x-ray spectroscopy (EDS) in a scanning electron microscope (SEM). In all cases, an excess of Ga is needed to form the MAX phase, which ends up diffusing to the surface of the film. This is consistent with other MAX phases, where an excess of the A-group element (*A*) is often critical [17,18].

Two representative films with different crystallographic orientations are discussed here (see below). Film 1 was grown with power values of 45 W for Mn, 10.6 W for Ga, and 206 W for C, giving an estimated atomic flux of 4.60×10^{14}, 3.55×10^{14}, and 2.35×10^{14} atoms/cm^2 s, respectively. The thickness of film 1 was estimated to be 375 nm. This estimation was achieved by growing a thinner film which was measurable by XRR and then scaling that thickness with the increased growth duration of the thicker film. Film 2 was grown with approximately 35% higher flux of Mn and C and 20% higher flux of Ga. Film 2 was estimated to be 140 nm by a similar process as before.

The structural properties of the films were investigated by x-ray diffraction using a Panalytical Empyrean diffractometer in line focus mode. For diffraction, the incident side had a two-bounce hybrid monochromator with a $1/8°$ divergence slit, and the diffracted side had a PIXcel^{3D} detector operating in one-dimensional (1D) mode. For pole figures, the same incident side optics were used, but a 0.04-rad Soller slit and a $0.27°$ parallel plate collimator were used on the diffracted side with the detector in open mode. The magnetic properties were measured by vibrating sample magnetometry (VSM) in the range from 3 to 320 K with a 5 T cryogen-free magnet system from Cryogenic.

III. RESULTS AND DISCUSSION

A. Film structure

Figure 1(a) shows x-ray diffraction (XRD) measurements for the two samples. Both films are an almost phase-pure Mn$_2$GaC MAX phase with film 1 only having very minor contaminants of Mn$_3$GaC and MnGa$_4$. These are thermodynamically stable competing phases which are often present in varying amounts in Mn$_2$GaC samples. The relative intensities of the Mn$_3$GaC and MnGa$_4$ peaks are consistent with randomly oriented polycrystalline phases. By comparing the area of the Mn$_3$GaC(1 1 1) and MnGa$_4$(2 2 0) peaks with that of the Mn$_2$GaC(0 0 0 6) peak, which are the 100, 100, and 18% relative intensity peaks of their respective phase, we can estimate that the concentration of Mn$_3$GaC is 0.024% and the concentration of MnGa$_4$ is 0.032%. Film 1 grows epitaxially with the (0 0 0 l) planes parallel to the MgO(1 1 1)
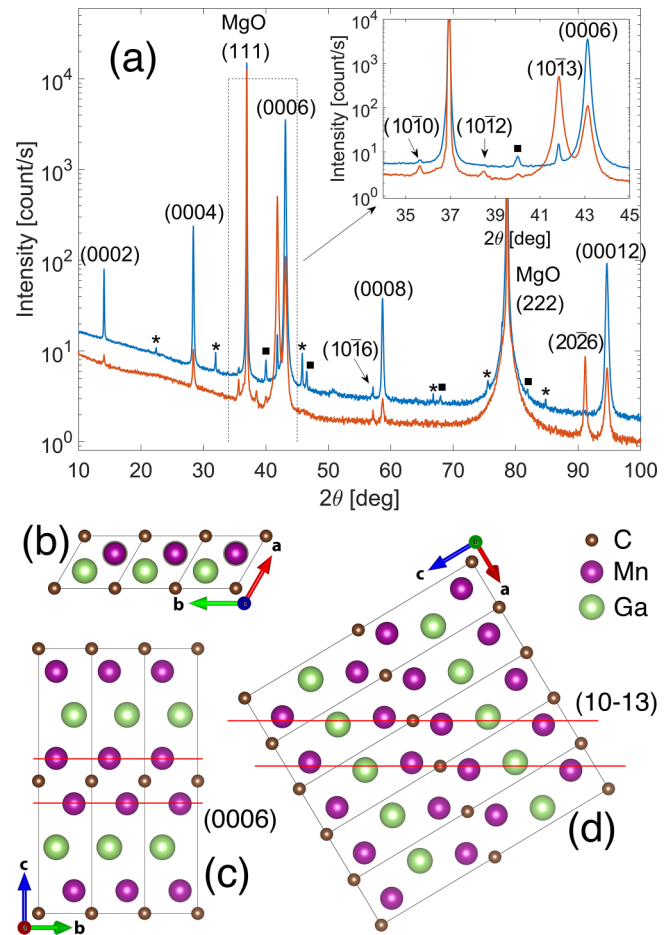

FIG. 1. (a) XRD scans of the two films, where the blue top curve is the single-orientation film and the red bottom curve is the mixed-orientation film. Peaks marked with a star are from MnGa$_4$, whereas squares are from Mn$_3$GaC. The inset is focused on the (0 0 0 6) and (1 0 $\bar{1}$ 3) peaks. Below are crystal structure schematics of Mn$_2$GaC: (b) and (c) have three unit cells visible, while (d) has six. (b) shows the top view, while (c) and (d) show the side views with the (0 0 0 6) and (1 0 $\bar{1}$ 3) lattice spacing highlighted, respectively.

planes. A very small peak corresponding to the (1 0 $\bar{1}$ 3) planes is also seen in film 1, indicating that 0.05% of grains grow with the (1 0 $\bar{1}$ 3) planes parallel to the MgO(111) planes. These "tilted grains" have been observed previously in other epitaxial MAX phase films such as Cr$_2$GeC [17]. The nucleation of (1 0 $\bar{1}$ 3) oriented grains probably occurs at film dislocations, which are ubiquitous due to the relatively large lattice mismatch between the film and the substrate. The adatom mobility and A-group element concentration could also be contributing factors [17]. Film 2 has no detectable contaminant phases but has a significant portion of (1 0 $\bar{1}$ 3) oriented grains parallel to the substrate surface. The relative x-ray peak intensities of the (1 0 $\bar{1}$ 3) and (0 0 0 6) planes are 100 and 18%, respectively. Integrating the area under the peaks, we can estimate that in film 2 the (1 0 $\bar{1}$ 3) oriented grains account for 51% of the film with 49% being (0 0 0 6). From reciprocal space map measurements (not shown) on film 1 we find that the lattice parameters are $c = 12.574 \pm 0.002$ Å and $a = 2.906 \pm 0.002$ Å, and for film 2 fitting the (1 0 $\bar{1}$ 3) and

(0 0 0 6) peaks in the XRD scan results in $c = 12.576 \pm 0.002$ Å and $a = 2.905 \pm 0.002$ Å. Both films have relatively large mosaicity, as seen by the full width at half maximum (FWHM) of the rocking curves on their principal peaks, which is around $1.3°$ (not shown) for both (0 0 0 6) peaks and $2.4°$ for the (1 0 $\bar{1}$ 3) peak. This is significantly larger than the FWHM of the MgO(111) rocking curve. However, we stress that both films are single-phase Mn_2GaC (discounting the minuscule amounts of impurity phases) and only the epitaxial relationship with the substrate differs. Film 1 we refer to as having a *single orientation*, whereas film 2 has *mixed orientations*.

Figures 1(b)–1(d) are schematics of the crystal structure of Mn_2GaC illustrating the M-A-M-X-M-A-M-X layered nature, drawn using the program Visualization for Electronic and Structural Analysis (VESTA) [19]. Figure 1(b) shows a top view of the unit cells, and Fig. 1(c) shows a side view, where the red lines indicate the distance between the (0 0 0 6) planes. Film 1 is almost entirely oriented with the c lattice vector of the MAX phase perpendicular to the film plane as shown in Fig. 1(c). The orientation of the tilted grains in film 2 is shown in Fig. 1(d), where the tilted (1 0 $\bar{1}$ 3) lattice planes are indicated with red lines. Film 2 is composed of grains with both (0 0 0 6) and (1 0 $\bar{1}$ 3) orientations.

Pole figures were obtained to examine the epitaxial relationship of the film and substrate further. The measurements were performed at $2\theta = 41.84°$, i.e., for the (1 0 $\bar{1}$ 3) planes, which are at an azimuthal angle of $\chi = 59.0°$ with respect to the (0 0 0 1) planes, as seen in Fig. 2(a). The single-crystal nature of film 1 can be seen from the discrete sixfold symmetric points. Film 2 in Fig. 2(b), which has a mixed orientation, has (1 0 $\bar{1}$ 3) peaks both in the center and at $\chi = 59.0°$. Additional peaks on both sides of the principal peaks can also be seen which are most likely a result of twinning. However, it should be noted that Fig. 2 is on a logarithmic scale and on a linear scale these additional peaks are barely visible with the peak in the center being dominant.

B. Magnetic properties

Mn_2GaC has a complex magnetic phase diagram which has been studied previously both experimentally and theoretically, but questions remain about the nature of the magnetic ordering at different temperatures [6,11,13,20,21]. Figure 3(a) shows the in-plane magnetic response of the single-orientation sample at high temperatures showcasing the metamagnetic transition. The inset shows out-of-plane measurements at the same temperatures. At low temperatures the film exhibits ferromagnetic-like (FM-like) behavior with a significant remanent magnetization of 0.18 μ_B/Mn atom. At $\sim$210 K a magnetic phase transition occurs to an antiferromagnetic (AFM) state, but a metamagnetic transition is observed at increasingly high fields with increasing temperature. These results are broadly the same as in previous studies, although the increased film thickness gives a significantly improved signal-to-noise ratio. The low amount of impurity phases (see above) means that their contribution to the measured magnetic signal is negligible. $MnGa_4$ has recently been shown to be antiferromagnetic with a Néel temperature of 393 K [22], but in the concentrations found here its magnetic signal is not measurable. Similarly, Mn_3GaC is known to be antiferromag-
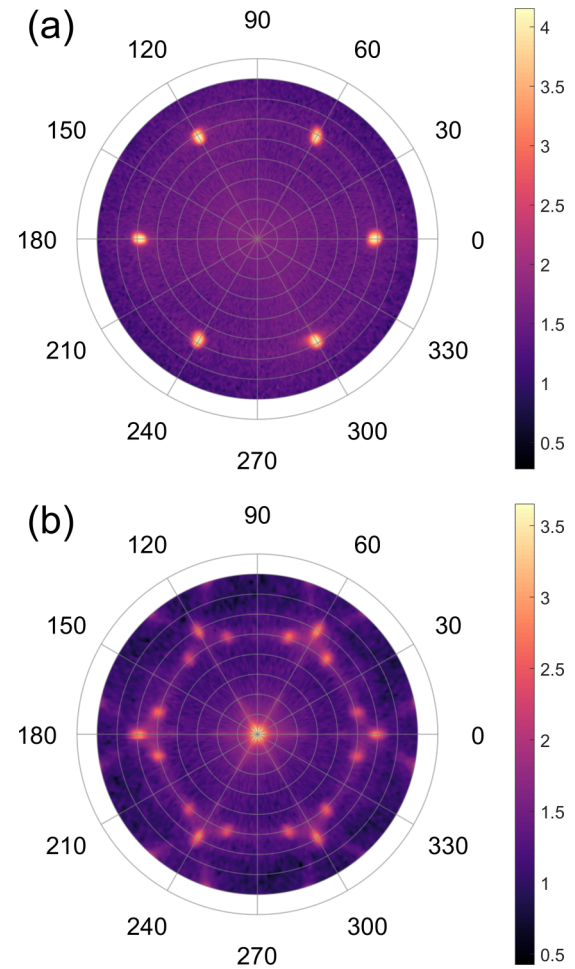

FIG. 2. Pole figures at $2\theta = 41.84°$ for the (1 0 $\bar{1}$ 3) peak of the films. (a) is a single orientation (0 0 0 6) film, while (b) has (1 0 $\bar{1}$ 3) and (0 0 0 6) mixed orientations. It should be noted that the intensity scale is logarithmic and in (b) most of the intensity is in the center spot.

netic below 170 K and then ferromagnetic between 170 and 270 K [23]. We do not see any clear signs of this in our data due to the minute amounts of Mn_3GaC in our samples. This, together with the near-single-phase nature of our films, means that the measured magnetic signal can only originate from the Mn_2GaC.

The magnetic model presented in Ref. [6] to explain the high-temperature regime is denoted as $AFM[0001]_4^A$ and has four adjacent Mn layers with collinear spins with a spin flip across every second Ga layer (the A layer). This is an AFM configuration with zero remanent moment. Theory suggests that the low-temperature magnetic state is a so-called canted $AFM[0001]_4^A$ state, where each block of four collinear Mn spins is canted by a small angle in the same direction, thus producing a net remanent magnetic moment at zero field. The AFM and canted AFM states are almost degenerate in energy for small angles, and therefore an applied magnetic field can nudge the system from fully AFM to canted AFM, which is the observed metamagnetic transition at high temperatures [6,16,24]. Ferrimagnetic ordering was also considered but was found to be less stable than both the FM and AFM
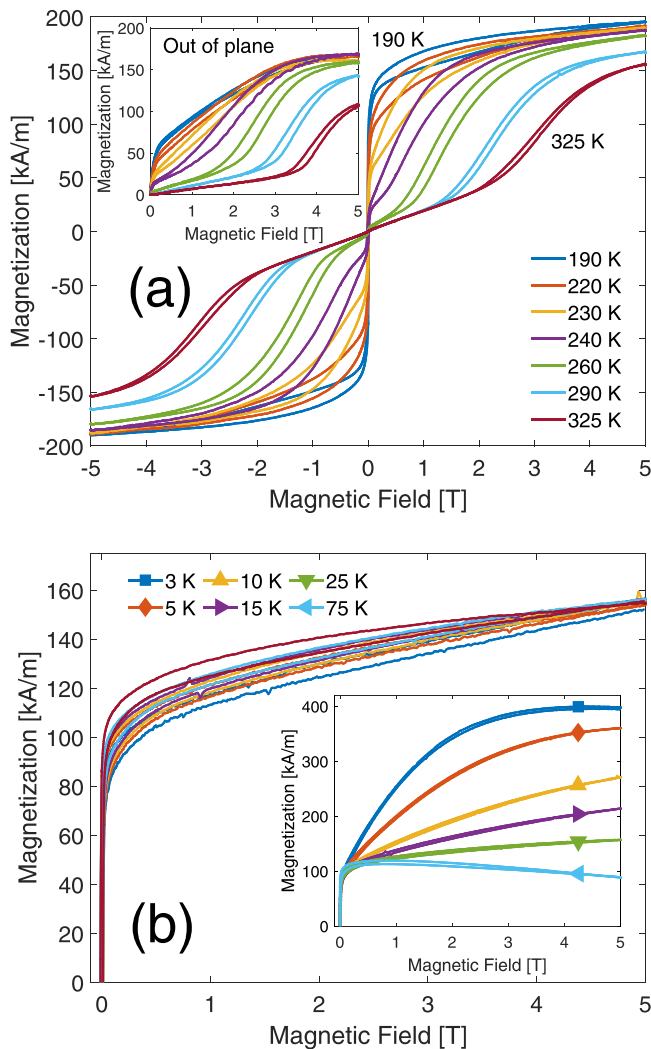
FIG. 3. (a) In-plane magnetization measurements for selected temperatures above the magnetic phase transition, with the inset showing out-of-plane measurements. All the measurements have had the MgO background subtracted. (b) Magnetization measurements at low temperatures (below the magnetic phase transition) with the background from the MgO substrate subtracted. The inset shows the raw measurements without background subtraction.

configurations [6]. However, a recent study has found that at low temperatures the coupling of the magnetic moments of the Mn across Ga layers is more complex than previously thought [14], and therefore there is still some doubt as to the precise magnetic ordering at low temperatures.

Previous studies have shown that the high-field magnetization (sometimes referred to as the saturation magnetization) increases sharply at temperatures below 50 K, which has been interpreted as an increase in the canting angle of the noncollinear AFM state [6]. However, low-temperature measurements of the magnetic properties of epitaxial Mn_2GaC films are complicated by the fact that the MgO substrate itself has a significant and increasing S-shaped magnetic response as the temperature is reduced below 50 K. This is due to magnetic impurities which are invariably present in single-crystal MgO substrates [5,6,11]. This means that to extract

the magnetic hysteresis loop of the film at low temperatures, it is necessary to account for the MgO background signal accurately. Figure 3(b) shows magnetization measurements between 3 and 75 K with the MgO background subtracted for the single-orientation film, while the inset shows the raw data. Background subtraction was done by measuring a MgO substrate from the same batch at the same temperatures as the film, and this signal was then subtracted from the film measurements. Care is needed to match the position and orientation of both film and substrate in the VSM, in order not to overcompensate or undercompensate the MgO contribution. Our results show that the magnetization at 5 T remains almost constant throughout this temperature range, at a value of 155 kA/m or 0.38 μ_B/Mn atom. This is contrary to what has been previously reported by Dahlqvist *et al.* [6], where an increasing magnetization was observed with decreasing temperature, up to 1.7 μ_B/Mn atom at 3 K and 5 T field, which is more than four times the magnetization seen here. However, since the thickness of the films studied here is almost four times larger than in previous studies, the background subtraction is much more robust, and therefore these results provide convincing evidence that the magnetization is in fact relatively constant over the entire low-temperature regime. This in turn shows that if the low-temperature state is that of canted AFM spins, the canting angle is constant with temperature.

Another hitherto unresolved question is that of magnetic anisotropy in MAX phases. MAX phases are naturally nanolaminated, which means that they have a highly anisotropic crystal structure. Theoretical calculations by Dahlqvist and Rosen [16] for Mn_2GaC predict that the easy axis is along the (0 0 0 1) planes and that the magnetic anisotropy energy can be affected by strain engineering [21]. Previous experimental studies of magnetism in MAX phases have been on either bulk samples with randomly oriented crystal grains or on epitaxial thin films with the *c*-axis perpendicular to the film plane [25]. Neither case is ideal for determining the magnetocrystalline anisotropy. Randomly oriented grains will give a net zero anisotropy, and in the epitaxial films the shape anisotropy is parallel with the Mn-C-Mn laminae, which means that it is impossible to separate shape anisotropy from magnetocrystalline anisotropy. Therefore the single-orientation and mixed-orientation films studied here present a unique opportunity to compare the magnetic responses along different well-defined crystallographic directions.

Figure 4 shows such a comparison of the magnetic response of the two films at 100 K when the field is applied parallel and perpendicular to the film plane. For the single-orientation film in Fig. 4(a) there is a considerable difference between in-plane (IP) and out-of-plane (OOP) measurements. The remanent magnetization is very small perpendicular to the film plane, and the magnetization at 5 T is also considerably smaller in the OOP direction. This is a fingerprint of in-plane magnetic anisotropy, but since the shape anisotropy favors in-plane magnetization, we cannot draw any conclusions about the possible contribution from magnetocrystalline anisotropy. The result for the mixed-orientation film [Fig. 4(b)] is strikingly different. Here the hysteresis curves are very similar in the IP and OOP directions, although the remanence is still greater in plane. From the structural characterization we
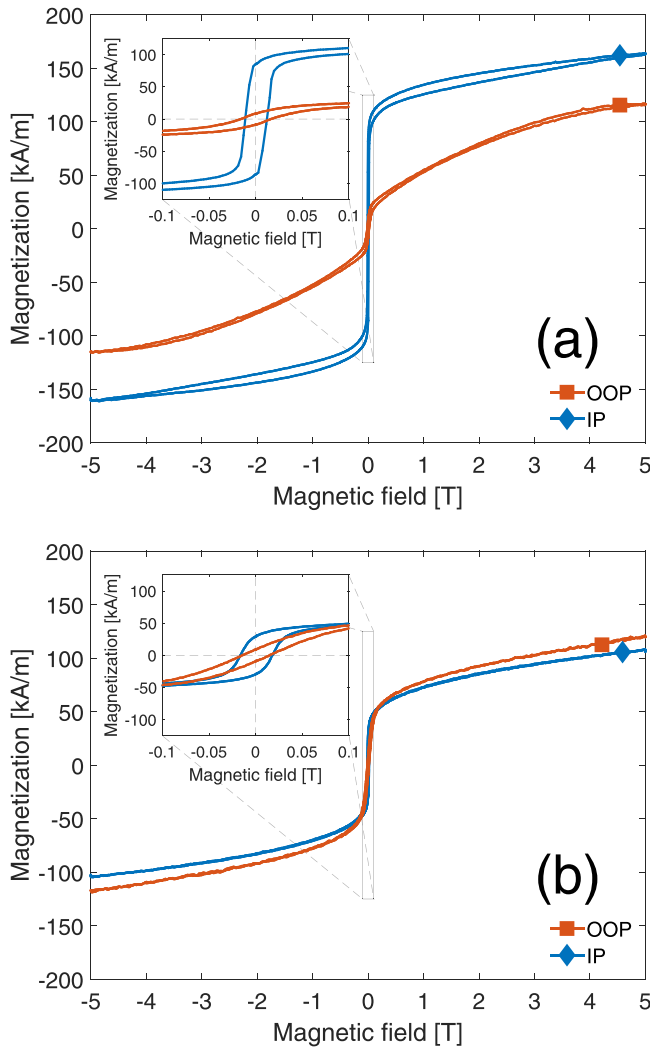
FIG. 4. Hysteresis measurements at 100 K. (a) and (b) show the in-plane and out-of-plane measurements of the single- and mixed-orientation films, respectively. The insets show a smaller field range around zero.
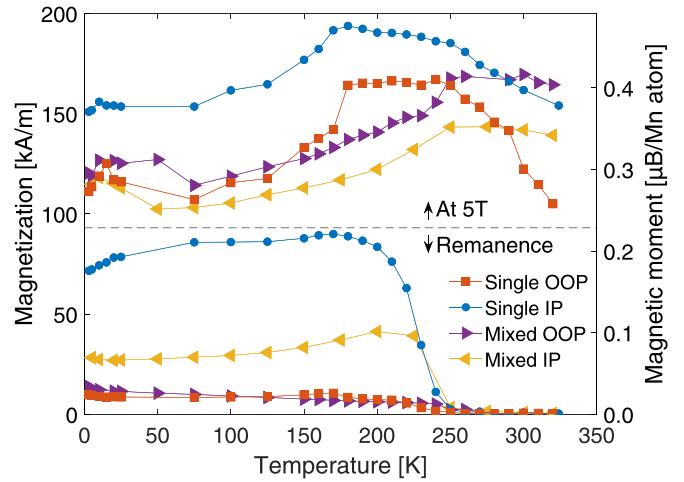

FIG. 5. Magnetization at 5 T and remanence as a function of temperature for the single- and mixed-orientation films in both in-plane and out-of-plane measurements.

estimated that 51% of the mixed-orientation film is composed of $(1\,0\,\bar{1}\,3)$ oriented grains which are at an angle of $59°$ with respect to the $(0\,0\,0\,1)$ planes. This means that in 51% of the film, the $(0\,0\,0\,1)$ planes are at an angle of only $31°$ with respect to the film normal, i.e., the OOP direction. It is clear that this has a significant effect on the magnetic response, lowering the energy barrier against rotating the magnetization perpendicular to the plane. This shows that Mn_2GaC has a magnetocrystalline anisotropy with $(0\,0\,0\,1)$ as the easy planes.

The same qualitative differences between IP and OOP magnetization in the single- and mixed-orientation films are observed over the entire temperature range studied. The mixed-orientation film has similar hysteresis loops IP and OOP, whereas the single-orientation film shows clear differences in magnetic response depending on whether the field is applied parallel or perpendicular to the $(0\,0\,0\,1)$ planes. This is also evident in the AFM high-temperature regime, where the metamagnetic transition occurs at a higher field in the OOP measurements, as can be seen in Fig. 3(a). It should be noted

that neither film appears to be fully saturated at the maximum field of 5 T, and this applies both IP and OOP.

Figure 5 shows the magnetization at 5 T as well as the remanence over the range 3–320 K. At the noncollinear to collinear AFM phase transition the remanence decreases sharply down to close to zero. The mixed-orientation film has considerably lower remanence in the IP direction than the single-orientation film over the whole range; however, both are similarly low in the OOP direction. The magnetization at 5 T is larger OOP than IP for the mixed-orientation sample which is opposite to what is observed for the single-orientation sample. As noted previously, this is because the mixed-orientation sample has a large fraction of $(1\,0\,\bar{1}\,3)$ oriented grains, which means that the $(0\,0\,0\,1)$ easy planes are closer to the OOP direction than the IP direction. The steep drop in magnetization in the single-orientation sample OOP is a manifestation of the metamagnetic transition shifting to fields above 5 T, which means that we are unable to complete the metamagnetic transition with the maximum available field.

IV. CONCLUSIONS

We have synthesized epitaxial films of Mn_2GaC with two different growth orientations on $MgO(1\,1\,1)$ substrates. The samples are either $(0\,0\,0\,1)$ dominated or a mix of $(0\,0\,0\,1)$ and $(1\,0\,\bar{1}\,3)$ orientations, as shown by detailed XRD characterization. Magnetization measurements were carried out in the range 3–320 K. By careful subtraction of the MgO background we were able to show that the high-field magnetization (at 5 T) is almost constant at temperatures below 50 K instead of increasing sharply, as has been previously reported, indicating a temperature-independent canting angle in the noncollinear AFM state. Comparison of the magnetic response of the differently oriented films shows that Mn_2GaC has a magnetocrystalline anisotropy with $(0\,0\,0\,1)$ as the easy planes, which is in agreement with theoretical calculations in the literature. These results demonstrate

how the nanolaminated structure of a MAX phase results in anisotropic magnetic properties. This key insight further secures the place of magnetic MAX phases among low-dimensional magnetic materials.

[1] N. Samarth, Magnetism in flatland, Nature (London) **546**, 216 (2017).

[2] B. Huang, G. Clark, E. Navarro-Moratalla, D. R. Klein, R. Cheng, K. L. Seyler, D. Zhong, E. Schmidgall, M. A. McGuire, D. H. Cobden, W. Yao, D. Xiao, P. Jarillo-Herrero, and X. Xu, Layer-dependent ferromagnetism in a van der Waals crystal down to the monolayer limit, Nature (London) **546**, 270 (2017).

[3] C. Gong, L. Li, Z. Li, H. Ji, A. Stern, Y. Xia, T. Cao, W. Bao, C. Wang, Y. Wang, Z. Q. Qiu, R. J. Cava, S. G. Louie, J. Xia, and X. Zhang, Discovery of intrinsic ferromagnetism in two-dimensional van der Waals crystals, Nature (London) **546**, 265 (2017).

[4] M. W. Barsoum, The $M_{N+1}AX_N$ phases: A new class of solids: Thermodynamically stable nanolaminates, Prog. Solid State Chem. **28**, 201 (2000).

[5] A. S. Ingason, A. Mockute, M. Dahlqvist, F. Magnus, S. Olafsson, U. B. Arnalds, B. Alling, I. A. Abrikosov, B. Hjörvarsson, P. O. Å. Persson, and J. Rosen, Magnetic Self-Organized Atomic Laminate from First Principles and Thin Film Synthesis, Phys. Rev. Lett. **110**, 195502 (2013).

[6] M. Dahlqvist, A. S. Ingason, B. Alling, F. Magnus, A. Thore, A. Petruhins, A. Mockute, U. B. Arnalds, M. Sahlberg, B. Hjörvarsson, I. A. Abrikosov, and J. Rosen, Magnetically driven anisotropic structural changes in the atomic laminate Mn_2GaC, Phys. Rev. B **93**, 014410 (2016).

[7] R. Meshkian, A. S. Ingason, U. B. Arnalds, F. Magnus, J. Lu, and J. Rosen, A magnetic atomic laminate from thin film synthesis: $(Mo_{0.5}Mn_{0.5})_2GaC$, APL Mater. **3**, 076102 (2015).

[8] A. Petruhins, A. S. Ingason, J. Lu, F. Magnus, S. Olafsson, and J. Rosen, Synthesis and characterization of magnetic $(Cr_{0.5}Mn_{0.5})_2GaC$ thin films, J. Mater. Sci. **50**, 4495 (2015).

[9] R. Salikhov, A. S. Semisalova, A. Petruhins, A. S. Ingason, J. Rosen, U. Wiedwald, and M. Farle, Magnetic anisotropy in the $(Cr_{0.5}Mn_{0.5})_2GaC$ MAX phase, Mater. Res. Lett. **3**, 156 (2015).

[10] A. Mockute, P. O. Å. Persson, F. Magnus, A. S. Ingason, S. Olafsson, L. Hultman, and J. Rosen, Synthesis and characterization of arc deposited magnetic $(Cr,Mn)_2AlC$ MAX phase films, Phys. Status Solidi RRL **8**, 420 (2014).

[11] A. S. Ingason, A. Petruhins, M. Dahlqvist, F. Magnus, A. Mockute, B. Alling, L. Hultman, I. A. Abrikosov, P. O. Å. Persson, and J. Rosen, A nanolaminated magnetic phase: Mn_2GaC, Mater. Res. Lett. **2**, 89 (2014).

[12] X. Z. Yu, Y. Onose, N. Kanazawa, J. H. Park, J. H. Han, Y. Matsui, N. Nagaosa, and Y. Tokura, Real-space observation of a two-dimensional skyrmion crystal, Nature (London) **465**, 901 (2010).

[13] I. P. Novoselova, A. Petruhins, U. Wiedwald, r. S. Ingason, T. Hase, F. Magnus, V. Kapaklis, J. Palisaitis, M. Spasova, M.

Farle, J. Rosen, and R. Salikhov, Large uniaxial magnetostriction with sign inversion at the first order phase transition in the nanolaminated Mn_2GaC MAX phase, Sci. Rep. **8**, 2637 (2018).

[14] J. Dey, M. Wójcik, E. Jędryka, R. Kalvig, U. Wiedwald, R. Salikhov, M. Farle, and J. Rosen, Non-collinear magnetic structure of the MAX phase Mn_2GaC epitaxial films inferred from zero-field NMR study (CE-5:L05), Ceram. Int. (2022).

[15] H. J. M. Jönsson, M. Ekholm, I. Leonov, M. Dahlqvist, J. Rosen, and I. A. Abrikosov, Correlation strength, orbital-selective incoherence, and local moments formation in the magnetic MAX-phase Mn_2GaC, Phys. Rev. B **105**, 035125 (2022).

[16] M. Dahlqvist and J. Rosen, Impact of strain, pressure, and electron correlation on magnetism and crystal structure of Mn_2GaC from first-principles, Sci. Rep. **10**, 11384 (2020).

[17] P. Eklund, M. Bugnet, V. Mauchamp, S. Dubois, C. Tromas, J. Jensen, L. Piraux, L. Gence, M. Jaouen, and T. Cabioc'h, Epitaxial growth and electrical transport properties of Cr_2GeC thin films, Phys. Rev. B **84**, 075424 (2011).

[18] A. S. Ingason, A. Petruhins, and J. Rosen, Toward structural optimization of MAX phases as epitaxial thin films, Mater. Res. Lett. **4**, 152 (2016).

[19] K. Momma and F. Izumi, VESTA3 for three-dimensional visualization of crystal, volumetric and morphology data, J. Appl. Crystallogr. **44**, 1272 (2011).

[20] S. Lyaschenko, O. Maximova, D. Shevtsov, S. Varnakov, I. Tarasov, U. Wiedwald, J. Rosen, S. Ovchinnikov, and M. Farle, Optical and magneto-optical properties of epitaxial Mn_2GaC MAX phase thin film, J. Magn. Magn. Mater. **528**, 167803 (2021).

[21] M. A. Vysotin, I. A. Tarasov, A. S. Fedorov, S. N. Varnakov, and S. G. Ovchinnikov, On the possible magnetic properties of ultrathin Mn_2GaC films on Al_2O_3 substrates, JETP Lett. **116**, 323 (2022).

[22] V. Y. Verchenko, A. A. Tsirlin, D. Kasinathan, S. V. Zhurenko, A. A. Gippius, and A. V. Shevelkov, Antiferromagnetic ground state in the $MnGa_4$ intermetallic compound, Phys. Rev. Mater. **2**, 044408 (2018).

[23] A. Petruhins, A. S. Ingason, S. Olafsson, and J. Rosen, Mn_3GaC inverse perovskite thin films by magnetron sputtering from elemental targets, Mater. Res. Express **7**, 106102 (2020).

[24] A. S. Ingason, G. K. Pálsson, M. Dahlqvist, and J. Rosen, Long-range antiferromagnetic order in epitaxial Mn_2GaC thin films from neutron reflectometry, Phys. Rev. B **94**, 024416 (2016).

[25] R. Salikhov, R. Meshkian, D. Weller, B. Zingsem, D. Spoddig, J. Lu, A. S. Ingason, H. Zhang, J. Rosen, U. Wiedwald, and M. Farle, Magnetic properties of nanolaminated $(Mo_{0.5}Mn_{0.5})_2GaC$ MAX phase, J. Appl. Phys. **121**, 163904 (2017).